Influence of Intermediate-Range Order on Glass Formation

Li Hui*

Physics Department, Trento University,I-38050, Trento, Italy

Received: October 3, 2003; In Final Form: January 14, 2004

The subpeak was first observed in glassy Fe−Al ribbons. The origin of the subpeak is not due to the system size, but it is consequence of the occurrence of local atomic structural order. The usual stability of undercooled liquids against crystallization is explained by means of local atomic structural order. Direct experiment shows a correlation between the nucleation barrier and intermediate-range order with decreasing temperature in an Fe−Al liquid. A corresponding simulation is used to observe the formation of the subpeak in a liquid system directly.

1. Introduction

Liquids usually solidify in two very different ways when they are cooled. The familiar route produces an ordered crystal with long-range order. An equally important one is disordered glass without long-range order. An understanding of the dynamics of supercooled liquids and glasses and whether the liquid−glass transition makes a subjacent thermodynamic phase transition still constitutes a challenge to condensed matter science.[1−4] Some important questions about freezing have remained unanswered. Experiments have not allowed us to measure directly how an atom moves to a particular neighbor in a solid or to observe which local structures are prone to reorganization. Therefore, a liquid-to-solid transition determined by experiment is hardly possible. Computer simulations provide an opportunity to study these processes at an atomic level. The use of molecular dynamics in the study of a hydrogen-bonded system was pioneered by Rahman and Stillinger in their famous paper on the simulation of liquid water.[5] Since then, this method has been applied to a variety of liquids. In recent times, there has been much progress in the understanding of the structure of liquids.[6−10] In a structural analysis, there is no doubt that the pair correlation function takes the chosen value. It yields basic information about the short-range order and serves as a key test for different structural models.[11] Mitral and co-workers[12,13] have used a two-body model with Coulombic interactions and a power-law repulsion, fitted to the short-range structure and melting temperature of cristobalite. Three-body forces have been introduced mainly to bring the bond-angle distributions into better agreement with the experimental data for the glass.[14] An optimized two-body potential developed by Tsuneyuki was applied with success to a study of a thermally induced phase transition in crystalline silica.[15] The effective pair potential was used to study the microstructure of amorphous Cr and Ga metals.[16,17] A molecular-dynamics simulation was used to simulate not only the glass-formation processes but also crystallization processes from the liquids. Stillinger and Laviolett reported local order in quenched states of simple atomic substances.[18] Watanabe and Tsumurava studied crystallization and glass formation in liquid sodium by the molecular-dynamics (MD) method.[19] The homogeneous nucleation of the crystalline phase from a supercooled liquid phase was studied for several model systems by means of the molecular-dynamics simulation. Hsu and Rahman reported the homogeneous nucleation and growth of a fcc crystalline phase with Lennard-Jones (LJ) 12−6 systems.[20] Several other fcc crystallization phase were observed in soft cores[21,22] and rubidium.[23] Moutain and Brown reported an observation of the bcc structure in a LJ system.[24] Hsu and Rahman observed the homogeneous nucleation and growth of a bcc structure in rubidium systems.[25] An analysis was made of the effect of the cooling rate,[26] the structural features of the glass,[27] the dynamics information of the system,[28,29] and the effects of boundary conditions.[20] However, until now, results in this research field have been insufficient. The link between local atomic structural order and the crystallization barrier for the solid phase was not experimentally established. As for the glass, a relevant question to ask in trying to characterize the structure of liquids and glasses is how the tetrahedrals are spatially correlated to each other in the structure. Complex interactions between atoms would determine the local atomic structure in a liquid. The cooperative phenomena of local structure play a dominant role in the structure and dynamics of liquids. Obviously, a better knowledge of these interactions will have important implications on the understanding of glass formation. The aim of this work is to analyze how the interaction determines the local structure and how the local structures affect the nucleation barrier.

2. Experimental Process and Simulation Method

2.1. Measurement of the Melt of the $Fe_{50}Al_{50}$ Alloy. In this paper, there are two sets of measurements: one is for the liquid, and the other is for the glasses. First, we describe the experimental process for the measurement of the liquid. An ingot of $Fe_{50}Al_{50}$ (50 at. % Fe and 50 at. % Al) was prepared by melting high-purity constituents (Al 99.999 wt %, Fe 99.9 wt %) in an Al_2O_3 crucible under an argon atmosphere. Measurements have been performed at constant temperatures of 1837, 1785, 1737, and 1647 K with the accuracy of ±5 K. The X-ray scattering experiment for the molten alloys were performed on a diffractometer equipped for Mo Kα radiation and a bent graphite monochromator. The intensity measurements were carried out by the $\theta-\theta$ step scanning method in the angular range of $5° \leq 2\theta \leq 90°$, which corresponds to the Q range of $5\ \text{nm}^{-1} \leq Q \leq 120\ \text{nm}^{-1}$. The scattering intensity measured in arbitrary units can be converted to the coherent scattering

* Corresponding author. E-mail: lihui@science.unitn.it.

10.1021/jp036968+ CCC: $27.50
Published on Web 04/06/2004

intensity per atom in electron units. The total structure factor can be obtained through equations

$$S(Q) = \frac{I_{\mathrm{eu}}^{\mathrm{coh}}(Q)}{\langle f^2(Q)\rangle}$$

$$\langle f^2(Q)\rangle = c_1 f_1^2(Q) + c_2 f_2^2(Q)$$

where $c_i = N_i/N$, N_i is the number of type-i atoms, and $f_i(Q)$ is the type-i atomic scattering factor. The pair correlation function $g(r)$ can be obtained by Fourier transition:

$$g(r) = 1 + \frac{1}{(2\pi)^3 n}\int \mathrm{e}^{-\mathrm{i}Qr}[S(Q) - 1]\,\mathrm{d}Q$$

2.2. Measurement of the Glassy $Fe_{50}Al_{50}$ Alloy. In this paper, amorphous ribbons are prepared by the single-roller melt−spinning technique under a partial argon atmosphere. The diameter of the copper roller was 35 cm, with a typical circumferential velocity of 40 m/s. The ribbons are 2 mm in width and 25 μm in thickness. The alloy was melted in an arc furnace and poured at temperatures of 1830, 1760, 1690, and 1640 K. To keep the Fe−Al glasses stable, small amounts of Ce elements were added to the Fe−Al alloy. The amorphous alloys have been investigated with X-ray wide-angle diffraction (XRD) using a $\theta-\theta$ diffractometer and Mo Kα radiation selected by a diffracted-beam focusing graphite monochromator. A standard treatment was applied to correct and normalize the experimental diffraction data and to obtain the pair correlation function $g(r)$.[30]

2.3. Simulation Method for the Cooling of the Liquid $Fe_{50}Al_{50}$ Alloy. In this simulation, the systems consisted of 1500 atoms subject to periodic boundary conditions. Two-component system (50% Fe and 50% Al atoms) are studied. In this paper, there are two simulations for the liquid. The first one is the simulation of an equilibrium liquid. The validity of the simulation is studied in the static simulation. As for the static simulation, the system is allowed to evolve for 8×10^4 time steps at a given constant temperature. The second one is to study the nonequilibrium properties of this well-characterized model. As for the second one, the strategy is the following: Starting from an equilibrium system at an initial temperature of 1955 K, we instantaneously quench the system by rescaling the particle velocities to a final temperature of 300 K at a quenching rate equal to 4.5×10^{13} K/s. The system is subsequently allowed to evolve at constant temperature for 5×10^4 time steps. This paper will make use of the n-body potential developed by Besson.[31] During each of these runs, 20 configurations are saved, 1 every 2000 time steps. In this paper, the time step is chosen to be 5×10^{-16} s. The volume of the simulated sample can be obtained on the basis of the experimental density of the materials. Here, the volume of the sample is 17.951 nm^3 for 1500 particles. The steepest-descent energy-minimization procedure with the conjugate gradient method, suggested by Stillinger and co-workers,[32,33] is imposed on each of these configurations to extract their inherent configurations, in which atoms are brought to the local minimum of the potential-energy surface.

3. Results and Discussion

3.1. Prepeak in the Experimental Structural Factor of the Liquid $Fe_{50}Al_{50}$ Alloy. The data analysis will be focused on the changes in chemical and topological intermediate-range order (IRO). The short-range order referred as SRO is rather well characterized in glasses. However, the question of the nature of the intermediate-range order (referred as IRO) in amorphous systems and its relationship to specific features is a more open subject. A peak emerging at a low wave vector in the structural factor of liquid FeAl systems, known as the prepeak, is observed in Figure 1, which is supposed to be related to a certain organization at intermediate distance in liquids. As shown in Figure 1, at $Q = 1.7$, the static structural factor exhibits a small but well-pronounced prepeak followed by the main peak. The prepeak occurs at a value of Q smaller than the position of the main peak of structural factor $S(Q)$. The prepeak is not due to the system size but is a consequence of complex chemical order. The interaction potential gives rise to the network structure that manifests the presence of the intermediate-range order. Also, Figure 1 shows that the temperature effect on the prepeak is very large. The height of the prepeak decreases as temperature increases. When the temperature reaches 1830 K, the prepeak disappears because of high temperature. This implies that high temperature weakens intermediate-range order. This observation of the prepeak is quite surprising. A clear prepeak distinguishes this liquid from all of the known common, simple liquids. This unique liquid would give rise to some novel glassy structures when it is quenched. This prepeak further enables us to ask what novel local structure would be produced in the glasses that resulted from this liquid with intermediate-range order.

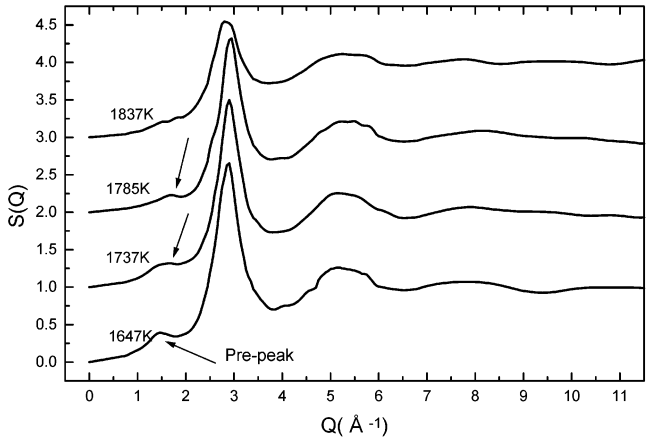

Figure 1. Prepeak in the experimental structural factors $S(Q)$.

3.2. Comparison between Simulation and Experiment. To be more precise, the theoretical pair correlation function is compared with the experimental result. An X-ray diffraction experiment has been done to test the validity of the simulation result. Results for the comparison of the simulated pair correlation function (PCF) and experimental data are given in Figure 2. The solid line represents simulated values, and the small dots represent the experimental results. As for a liquid, the pair correlation function is the only parameter that can be measured by experiment. Thus, the validity of the simulation carried out on the liquid can be checked by an X-ray experiment on $g(r)$. Figure 2 shows that our simulations at 1623, 1647, and 1737 K are in good agreement with the experiments. The positions of the theoretical peaks agree with the positions of the experimental peaks very well, and the magnitudes of these peaks are also quite close to the experimental values. However, the height of the first peak in $g(r)$ at 1785 and 1837 K are slightly underestimated as compared to experiments, but the second and the third peaks are much closer to the experimental curves. The overall agreement between simulation and experiment is rather good. Such a straightforward comparison with experiment also proves that this potential used in our simulation can accurately describe the structural features of the liquid FeAl

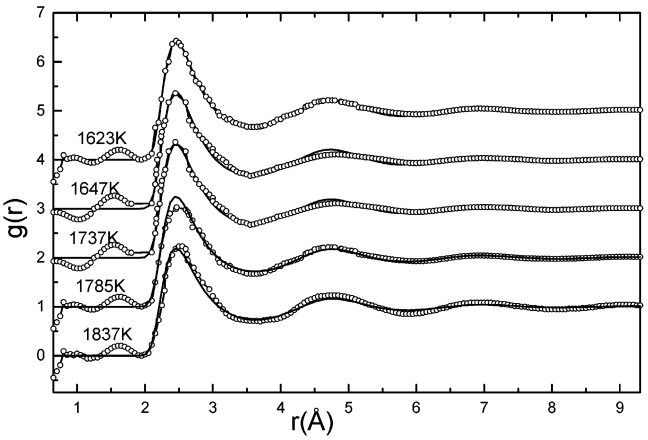

Figure 2. Results for comparison between the experiment and static simulations on a liquid. (○) Experimental results; (—) static simulation results.

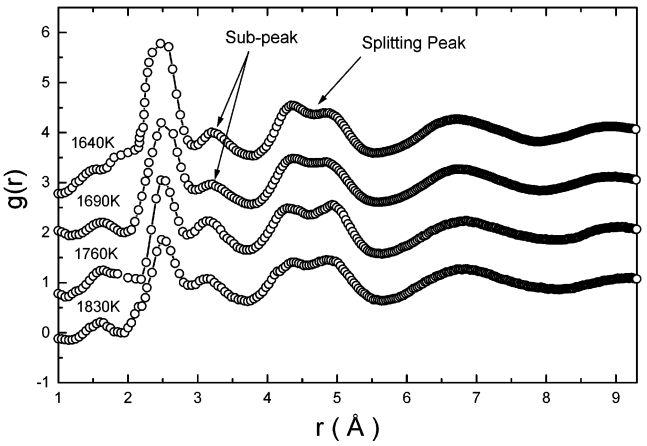

Figure 3. Subpeaks in experimental pair correlation functions of glassy ribbons.

alloy. Having established the reliability of our simulation, we will carry out a series of simulations for the study of our interesting problems.

3.3. Subpeak in the Experimental PCF of the Glassy Ribbons. The prepeak has been observed in the liquid Fe−Al alloy. What then is the effect of the prepeak on the glassy structure of the FeAl alloy? To answer this question, the novel microstructure in the glassy Fe−Al alloy must be observed directly. This is what we want to study in this paper. Figure 3 shows the experimental pair correlation function from the scattering data for the glassy Fe−Al ribbon as a function of pouring temperature. The obvious splitting of the second peak of $g(r)$ gives strong evidence of an amorphous structure. The most interesting aspect of the experimental data is the enhancement of a subpeak (more clearly visible in Figure 3) on the right-hand of the main peak in the pair correlation function. This subpeak is also observed in many different samples of similar composition. This subpeak is responsible for the local atomic structural order in glassy Fe−Al. The increasing distinction of the subpeak with decreasing pouring temperature demonstrates that the local order in the glasses becomes better defined and more pronounced at lower temperatures, confirming predictions made by Steinhardt et al.[34] This subpeak is consistent with interpenetration of local icosahedral order. The development of the subpeak on the right of the main peak further indicates that it reflects growing local topological order. However, no subpeak is observed in the statistic pair correlation

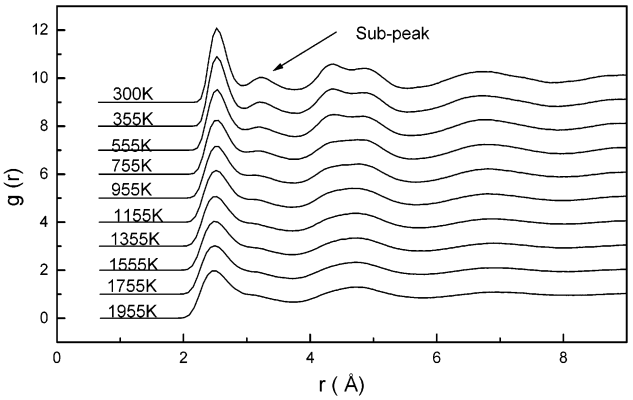

Figure 4. Simulated subpeaks in pair correlation functions on cooling of the 1500-atoms system.

function of the liquid Fe−Al alloy by experiment (shown in Figure 2). The local atomic structure in the liquid Fe−Al alloy is not similar to that of the quenched glassy Fe−Al alloy. This result further shows that quenching cooling results in the subpeaks. What local atomic structure does give rise to the subpeaks in the pair correlation function in the cooling process? The results presented below provide some description of the local atomic structures in the process of glass formation.

3.4. Simulation Results for the Cooling of the Liquid $Fe_{50}Al_{50}$ Alloy. In a liquid, it may be assumed that tightly bound, closely packed clusters dominate the subpeak in the pair correlation function, allowing further investigations of the origin of the subpeaks by molecular dynamics simulations. Experiments have not allowed us to observe directly the process of local atomic order formation. Therefore, the origin of the subpeak determined by experiment is hardly possible. Molecular dynamics simulations can generate realistic structural models for materials and provide dynamics information about glass formation. Here we report the results of extensive simulations of the cooling of Fe−Al alloys at constant pressure.

Figure 4 shows the results for the simulated pair correlation function on cooling. The obviously splitting of the second peak is immediately noticed in the pair correlation function, indicating glass formation in the system. Even more dramatic, on the right-hand of the main peak in the pair correlation function, we found a subpeak around $R = 0.32$ nm. Interestingly, with decreasing temperature, the height of the subpeaks increases. The subpeak incidentally becomes more pronounced, and at $T = 300$ K, it becomes a clearly independent peak. The subpeak is very similar to the ones seen in the glassy ribbon , as mentioned above for Figure 3. The process of the subpeak's formation is clearly seen from these growing pair correlations on cooling. The subpeak, prominent in the experimental data, is reproduced in the calculated $g(r)$ from the simulation when the cooling effect is considered. The simulation results account for the subpeak. If no cooling effect is considered, then it is certain that the subpeak is not observed in the pair correlation function, particularly at low temperatures, contrary to the experimental results. At high temperatures, kinetic energy is prevalent; however, the chemical potential is in second place. Therefore, the local order is destroyed, and the subpeak cannot be observed. With decreasing temperature, the chemical potential is inclined to be in first place and chemical order results in local structure formation, so the subpeak occurs. The obvious subpeak found in the PCF makes us assume the presence of a new, strong local atomic structural order in the glass. The IRO would be screened by the chemical ordering of different atomic species. The intermediate-range

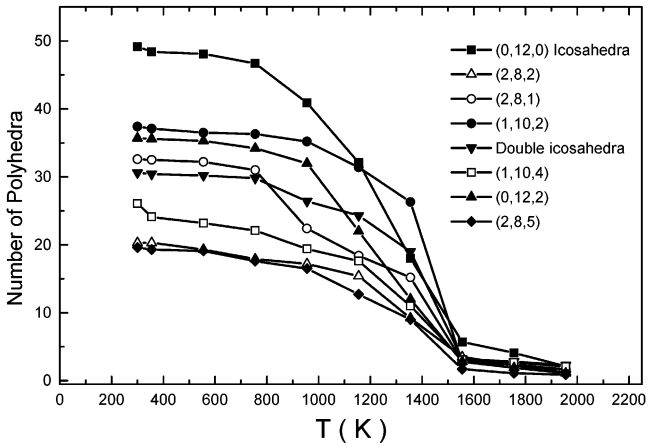

Figure 5. Defective icosahedra and ideal icosahedron on cooling.

order and geometrical structure are responsible for the subpeak. To confirm this hypothesis, we try in this paper to analyze local clusters and polyhedra in glasses.

Now we clarify the above aspects. For this, all canonical Frank−Kasper polyhedra and a number of defective icosahedra are detected and counted in simulated liquids and glasses. The Honeycutt−Anderson[35,36] index gives us an opportunity to define icosahedron, FK, Bernal, and other defective icosahedra in a very simple and precise way. For convenience, we use a signature to represent our defective icosahedra. The first index in the signature is the number of 1441 bonds, the second index is the number of 1551 bonds, and the third index is the number of 1661 bonds. For example, if and only if the central atom has 14 neighboring atoms, 12 of which are joined to the central atom by 1551 bonds and two of which are joined to the central atom by 1661 bonds, then they define an FK polyhedron with a coordination number of $Z = 14$. In the same way, other polyhedra can be defined. Figure 5 shows the numbers of different kinds of polyhedra in the inherent structures as a function of temperature on cooling. None of the types of polyhedra shows any significant change as the temperature is varied over the range of $T > 1355$ K. We therefore find that the structure undergoes no large changes with temperature at high temperatures. At low temperatures, however, there is a substantial increase in all types of polyhedra. The structural-transition temperature is identical to the temperature of subpeak formation in Figure 4. A polyhedron consisting of some 1551, 1661, and/or 1441 clusters is called a defective icosahedron. As shown in Figure 5, (0, 12, 3) polyhedra, made of twelve 1551 bonds and three 1661 bonds, and (0, 12, 4) polyhedra, composed of twelve 1551 bonds and four 1661 bonds, are detected. Bernal canonical (2, 8, 4) hole polyhedra, composed of eight 1551 bonds, two 1441 bonds, and four 1661 bonds, are found. Defect (1, 10, 2) icosahedra, characterized by ten 1551 bonds and one 1441 bond interposed between two 1661 bonds, are observed in the system. The structure of the Fe−Al component glass is predominantly icosahedra. We found 49 icosahedra in a sample of 1500 atoms, with 60% of the atoms in icosahedra. On average, each icosahedron interpenetrates 2.2 and shares a face with 2.0 other icosahedra. This suggests that the tendency to form icosahedral structures would be even greater in macroscopic systems. Not only ideal icosahedra but also a variety of defective icosahedra were detected. All icosahedra and defective icosahedra interpenetrate and share faces and vertexes with other icosahedron and defective icosahedron. The novel subpeaks result from the interpenetration of icosahedra and defective icosahedra.

It is worth noticing that the size effect is very important to the simulation result, although the periodic boundary condition can be used to reduce the size and surface effects. In fact, Honeycutt and Andersen investigated the size effect on crystal nucleation in supercooled liquids.[37] In general, in the absence of small-system-size artifacts, the number of particles in the critical nucleus for a given choice of cutoff angle should be independent of system size. However, Honeycutt and Anderson found that the mean number of particles in the critical nucleus for larger systems is considerably greater than that for the smaller systems. This is in contrast to what is expected in the absence of small-system-size artifacts, where the number of particles in the critical nucleus should be independent of system size. Honeycutt's result indicated that small system size disrupted the normal critical nucleus formation. There is a possibility of small-system-size effects other than those due to the presence of periodic boundary conditions. In our present simulation, the size effect is also observed. The percentage of the local clusters and the PCF for $N = 1500$ is different with that for $N = 500$. Because we paid attention to the size effect on the simulation result, 1500 particles are used in this simulation of other than 500 particles. Although the size effect is great, the present simulation gives some important information.

During the cooling process, crystal nucleation and icosahedral ordering are two competing tendencies with a smaller time scale in the two component liquids, and we find clear anticorrelation between the crystal pairs and the icosahedral pairs in the low-temperature configurations obtained. In the cooling process, the IRO coupled with the nucleation barrier for crystallization. An increasing IRO in an FeAl liquid with undercooling is manifested by a subpeak. Furthermore, we show that this increasing IRO is responsible for the nucleation of the undercooled liquid FeAl. The icosahedral structure signals a smaller nucleation barrier, indicating that the intermediate-range order of the liquid is similar to that of the icosahedral structure. These results demonstrate the connection between the local atomic structural order of the liquid and the nucleation barrier. That the development of regions of intermediate-range order in the liquid is critical to the nucleation of ordered phases with similar IROs blurs the distinction between homogeneous and heterogeneous nucleation in these cases and indicates that local order is important and must be considered in nucleation theories.

All thermodynamic models for nucleation predict that new clusters in the liquid must reach a specific critical size before they are biased to grow rather than dissolve; the critical size is inversely proportional to the driving free energy. Because the data in Figures 3 and 4 demonstrate that, at least in this alloy, icosahedral order already exists above the liquid temperature, the relative length scales of the critical cluster size and the coherence length of the order in the liquid must be important. As the temperature of the liquid is decreased, nucleation becomes possible below its metastable liquidus temperature because of a growing coherence length in the liquid and a decreasing critical size. The liquid/cluster interface is certainly more diffuse than assumed with classical theory;[38] such similar length scales clearly suggest that the structural fluctuations in the liquid act as a template, decreasing the barrier for nucleation and blurring the distinction between the homogeneous and heterogeneous nucleation of ordered phases.

4. Conclusions

To summarize, we have demonstrated enhanced icosahedral intermediate-range order with undercooling in FeAl liquids that

form icosahedral structures. The origin of the barrier to nucleation of crystallographic phases is the formation of local icosahedral order in the liquid. The data presented demonstrate that the local order in the liquid strongly influences the nucleation of the specific phases. The influence of preexisting local order in the liquid is an important ingredient in the liquid/solid phase transition that should be considered in theoretical treatments of nucleation.

Acknowledgment. This work is supported by the National Natural Science Foundation (NSF) (grant nos. 29890210, 50071028, and 50231040) and in part by the Natural Science Foundation (NSF) of Shandong province (grant no. L2001F01).

References and Notes

(1) Mandell, M. J.; Mctague, J. P. *J. Chem. Phys.* **1976**, *64*, 3699.
(2) Mandell, M. J.; Mctague, J. P. *J. Chem. Phys.* **1977**, *66*, 3070.
(3) Li, D. H.; Moore, R. A.; Wang, S. *J. Chem. Phys.* **1988**, *89*, 4309.
(4) Nakano, H.; Qi, D. W.; Wang, S. *J. Chem. Phys*. **1989**, *90*, 1871.
(5) Rahman, A.; Stillinger, F. H. *J. Chem. Phys.* **1971**, *55*, 3336.
(6) Mezard, M.; Parisi, G. *J. Chem. Phys.* **1999**, *111*, 1076.
(7) Coluzzi, B.; Parisi, G.; Verrocchio, P. *J. Chem. Phys.* **1999**, *111*, 9039.
(8) Tostmann, H.; Dimasi, E.; Pershan, P. S.; Ocko, B. M.; Shhpyrko, O. G. *Phys. Rev. B* **2000**, *16*, 7284.
(9) Kob, W.; Barrat, J.-L. *Phys. Rev. Lett*. **1997**, *78*, 4581.
(10) Coluzzi, B.; Parisi, G.; Verrocchio, P. *Phys. Rev. Lett*. **2000**, *84*, 306.
(11) Jin, W.; Kalia, R. K.; Vashishta, P. *Phys. Rev. B* **1994**, *50*, 118.
(12) Mitra, S. K.; Amini, M.; Fincham, D. Hockney, R. W. *Philos. Mag.* **1981**, *43*, 365.
(13) Mitra, S. K. *Philos. Mag*. **1983**, *47*, L63.
(14) Mozzi, R. L.; Warren, B. E. *J. Am. Ceram. Soc*. **1969**, *2*, 164.
(15) Tsuneyuki, S.; Aoki, H.; Tsukada, M. *Phys. Rev. Lett.* **1990**, *64*, 776.
(16) Lai, S. K.; Wang, S.; Wang, K. P. *J. Chem. Phys*. **1987**, *87*, 599.
(17) Tsay, S. E. *Phys. Rev. B* **1993**, *48*, 5945.
(18) Stillinger, F. H.; Laviolette, R. A. *Phys. Rev. B* **1986**, *34*, 5136.
(19) Watanabe, M. S.; Tsumuraya, K. *J. Chem. Phys.* **1987**, *87*, 4891.
(20) Hsu, C. S.; Rahman, A. *J. Chem. Phys.* **1979**, *71*, 4974.
(21) Tanemura, M.; Hiwatari, Y.; Matsuda, H.; Ogawa, T.; Ogita, N.; Ueda, A. *Prog. Theor. Phys.* **1977**, *58*, 1079.
(22) Cape, J. N.; Finney, J. L.; Woodcock, L. V. *J. Chem. Phys.* **1981**, *75*, 2366.
(23) Mountain, R. D.; Basu, P. K. *J. Chem. Phys.* **1983**, *78*, 7318.
(24) Mountain, R. D.; Brown, A. C. *J. Chem. Phys*. **1984**, *80*, 2730.
(25) Hsu, C. C.; Rahman, A. *J. Chem. Phys.* **1979**, *70*, 5234.
(26) Vollmayr, J. *Chem. Phys.* **1996**, *105*, 4714.
(27) Rose, J. P.; Berry, R. S. *J. Chem. Phys*. **1992**, *96*, 517.
(28) Martyna, G. J.; Klein, M. L. *J. Chem. Phys.* **1992**, *97*, 2635.
(29) Evans, D. J. *J. Chem. Phys.* **1983**, *78*, 3297.
(30) Cormier, L.; Ghaleb, D.; Delaye, J. M.; Calas, G. *Phys. Rev. B* **2000**, *61*, 14495.
(31) Besson, R.; Morillo, J. *Phys. Rev. B* **1997**, *55*, 193.
(32) Stillinger, F. H.; Weber, T. A. *Phys. Rev. A* **1982**, *25*, 978.
(33) Stillinger, F. H.; Laviolette, R. A. *Phys. Rev. B* **1986**, *34*, 5136.
(34) Steinhardt, P. J.; Nelson, D. R. *Phys. Rev. Lett.* **1984**, *53*, 1947.
(35) Honeycutt, J. D.; Anderson, H. C. *J. Phys. Chem.* **1987**, *91*, 4950.
(36) Frank, F. C.; Kasper, J. S. *Acta Crystallog.* **1958**, *11*, 184. Frank, F. C.; Kasper, J. S. *Acta Crystallog.* **1959**, *12*, 483.
(37) Honeycutt, J. D.; Andersen, H. C. *J. Phys. Chem.* **1986**, *90*, 1585.
(38) Kelton, K. F. In *Solid State Physics*; Ehrenreich, H., Turnbull, D., Eds.; Academic Press: Boston, 1991; p 75.